hydrology

MDPI

Article

Analyzing Multisource Hydrological Variability for Precise Water Allocation in an Arid Terminal Lake: A Case Study of Taitema Lake, Northwest China

Shuo Zhang [1], Guang Yang [1,*], Yun Zhang [2] and Hongbo Ling [2,*]

[1] College of Water Conservancy and Architectural Engineering, Shihezi University, Shihezi 832000, China
[2] Key Laboratory of Ecological Safety and Sustainable Development in Arid Lands, Xinjiang Institute of Ecology and Geography, University of Chinese Academy of Sciences, Urumqi 830011, China
* Correspondence: yangguang@shzu.edu.cn (G.Y.); linghb@ms.xjb.ac.cn (H.L.)

Abstract

Terminal lakes in arid regions are highly vulnerable to climate variability and human water management, yet their long-term hydrological responses under multi-river regulation remain insufficiently quantified. Using Taitema Lake at the terminus of the Tarim Basin as a case study, this research integrates Landsat and Sentinel observations (2005–2025) with meteorological and river-inflow records to examine lake area dynamics and to identify river-specific hydrological controls. The results show pronounced intra- and interannual variability, with the lake expanding to a maximum of 461.52 km^2 in October 2017 and shrinking to 0.35 km^2 in October 2008. High-frequency permanent water (~43 km^2) is concentrated in the deep central basin and largely influenced by the Qarqan River, whereas seasonal water (~300 km^2) is broadly distributed and strongly affected by ecological releases from the Tarim River. Quantified inflow–area relationships indicate that the lake expands by 7–14 km^2 for each 0.1 × 10^8 m^3 of inflow. Based on frequency-based hydrological analysis, this study develops joint inflow strategies for wet, normal, and dry years, offering a practical hydrological basis for more precise and adaptive water allocation schemes in arid terminal lakes.

Keywords: Taitema Lake; terminal lake; arid region; ecological water conveyance; hydrological variability; water body extraction; remote sensing; joint water resources management; Tarim River; Qarqan River

Check for updates

Academic Editor: Ali A. Assani

Received: 1 December 2025
Revised: 23 January 2026
Accepted: 26 January 2026
Published: 28 January 2026

Copyright: © 2026 by the authors. Licensee MDPI, Basel, Switzerland. This article is an open access article distributed under the terms and conditions of the Creative Commons Attribution (CC BY) license.

1. Introduction

Terminal lakes and wetlands are the primary and essential carriers of surface water resources in arid regions and constitute crucial components of oasis ecosystems [1]. They perform multiple ecological functions, including water-cycle regulation, biodiversity support, and desertification control, making them indispensable to the survival of both humans and natural ecosystems within a basin [2,3]. In addition to being vital resources for human activities and livelihoods, terminal lakes and wetlands also serve as sentinels of global climate change [4,5]. Owing to their location in an extremely fragile zone of "water–air–land" interaction, they are highly sensitive to climate disturbances and human activities [2], and can provide early and clearer signals of environmental change [6]. In recent decades, as climate change has intensified and human activities have increased, the spatial locations and morphologies of many terminal lakes in arid regions have undergone substantial transformations, with many shrinking drastically or even disappearing [7,8].

Therefore, to ensure the rational and efficient allocation of water resources in arid regions, it is necessary to monitor the long-term and dynamic changes in terminal lake wetlands in a continuous and timely manner [9].

Currently, the main methods for water body extraction based on remote sensing data include band thresholding, water index–based approaches, and machine learning methods [10–12]. Advances in remote sensing technology have greatly enhanced our understanding of the Earth's surface. By regularly acquiring satellite imagery, it is possible to monitor dynamic changes in the surface environment in an efficient and timely way [13,14]. Remote sensing and GIS technologies are now widely applied in water resources monitoring. Due to their synoptic coverage, dynamic capability, and cost-effectiveness, remote sensing data can provide rapid and accurate lake surface information at relatively high temporal frequencies, thereby offering strong support for analyzing the spatiotemporal evolution of lake extents [10,15]. Surface water dynamics can be monitored using optical remote sensing with various spatial resolutions, such as the MODIS series, Landsat series, Sentinel-2, and Gaofen series [16–18]. In addition, microwave remote sensing sensors, such as Sentinel-1 and the Jason series, are less affected by cloud cover and illumination conditions and show a reduced sensitivity to vegetation cover, making them suitable for monitoring water level changes and flood dynamics [19,20]. In this study, Landsat series and Sentinel-2 imagery are used to monitor and extract the lake surface area of Lake Taitema from 2005 to 2025.

Over the long term, substantial research progress with significant academic value and practical relevance has been achieved regarding watershed-scale surface water extraction methods, spatiotemporal evolution patterns, and analyses of driving mechanisms [21–23]. As the terminal lake of both the Tarim River—the largest inland river in China—and the Qarqan River, Lake Taitema constitutes a crucial component of the downstream ecosystems of these two rivers and serves as a key indicator of climate change. The lake possesses both considerable potential for resource development and unique ecological value [16,24]. Since the 1970s, population growth along both banks of the Tarim River, intensified human activities, and increasingly frequent extreme climatic events have led to the drying up of the river's downstream reach in 1972, which in turn caused progressive degradation and eventual desiccation of Lake Taitema, accompanied by a continual deterioration of its natural environment [25,26]. With growing national attention to ecological degradation in the region, a total of 26 ecological water releases have been implemented to the lower Tarim River from 2000 to April 2025. Under this sustained intervention, the wetland area of Lake Taitema has gradually recovered, groundwater levels have risen significantly, and the ecological environment has improved markedly [27,28].

This transformation has attracted extensive attention from scholars, with research topics covering the lake surface dynamics of Lake Taitema since the initiation of ecological water conveyance, variations in groundwater levels, vegetation responses, and overall ecological feedbacks and habitat-quality assessments of the ecosystem [29–31]. Since the start of ecological water conveyance, the spatial distribution of water bodies has shifted from a western-dominated pattern to one characterized by greater water coverage in the east and increasing hydrological connectivity, accompanied by an overall eastward migration of the lake area centroid. Existing studies indicate that the Qarqan River provides a more substantial and stable contribution to the replenishment of Lake Taitema; moreover, the two rivers exhibit markedly different lead–lag patterns in their runoff processes, with the main periodicity of the Tarim River occurring at 2.9 years, while that of the Qarqan River is 5.7 years. The probability of synchronous wet–dry conditions between the two rivers is 44.52%, whereas asynchronous conditions occur with a probability as high as 55.48% [6]. Other studies have developed a priority framework for vegetation protection in the Lake Taitema region, identifying the

spatial distribution and extent of different vegetation types and providing an effective basis for targeted conservation practices [32]. However, although substantial research has been conducted on the spatiotemporal evolution of Lake Taitema's surface area and the hydrological characteristics of inflows from the Tarim and Qarqan rivers, detailed analyses of how the lake surface evolves dynamically under the combined influences of the two rivers, as well as the specific regions of the lake controlled, respectively, by each river, are still lacking. To achieve precise water allocation and joint water resources management for Lake Taitema, further in-depth investigation is urgently needed to address these key scientific questions.

The objectives of this study are fourfold: (1) to extract a monthly lake water body dataset covering the past two decades using high-precision, long-term remote sensing imagery on the Google Earth Engine (GEE) platform; (2) to investigate the spatiotemporal variations in Lake Taitema from 2005 to 2025; (3) to track the dynamic evolution of the lake surface under inflows from the two rivers, quantify the relationship between inflow volume and lake surface area, and delineate the respective control regions governed by each river; and (4) to develop ecological regulation schemes for the joint water resources management of the two rivers under years with different occurrence probabilities, thereby achieving precise water allocation for Lake Taitema.

2. Materials and Methods

2.1. Study Area

Lake Taitema is located in the southeastern Tarim Basin in China, within a desert-encircled zone bordered by the Taklimakan Desert to the west and the Kumtag Desert to the east [33]. The associated wetland system provides an indispensable stopover and habitat for migratory birds. The terrain around the lake is low-lying and flat, and the lake itself is very shallow, with an average water depth of only 0.4–0.7 m. The region is characterized by a temperate continental arid climate, with annual precipitation of less than 50 mm and extremely high annual evaporation of 2500–3000 mm [34]. Surface water in the lake–wetland area is supplied primarily by ecological water releases from the lower Tarim River and downstream ecological discharges from the Qarqan River [35] (Figure 1).

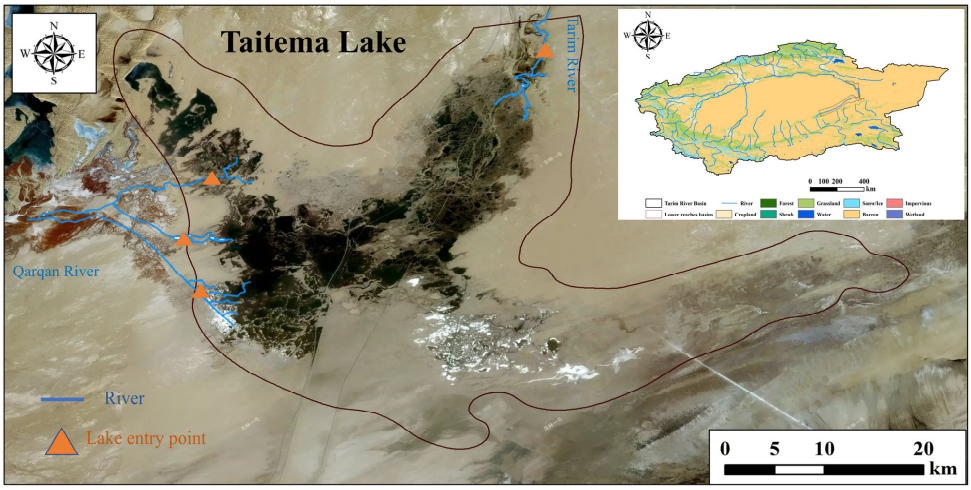


Figure 1. Location of the study area.

The lower Tarim River, commonly referred to as a "green corridor," extends for more than 360 km from the Daxihaizi Reservoir to Lake Taitema, with extensive desert riparian forests distributed along both banks. These forests form a crucial ecological barrier that effectively prevents the Taklimakan and Kuruk deserts from converging [36,37]. The lower Qarqan River stretches for over 300 km from the Tatirang Bridge to Lake Taitema, and its

channel largely maintains a natural geomorphic state as it traverses the desert zone. As the terminal lake jointly fed by the Tarim and Qarqan rivers, Lake Taitema exhibits pronounced spatiotemporal fluctuations in lake surface patterns at both intra-annual and interannual scales, driven by the combined influences of ecological water releases from the Tarim River, ecological discharges from the Qarqan River, and strong lake evaporation [38,39].

2.2. Data Sources

This study employs multisource, multi-temporal satellite imagery to capture the annual, monthly, and sub-monthly dynamics of lake surface changes in the study area from 2005 to 2025. In addition, meteorological observations, discharge measurements provided by the Tarim River Basin Authority, inflow volumes, and other ecological water data are integrated for comprehensive analysis.

Lake surface remote sensing data: Landsat TM/OLI series imagery from 2005 to 2025 (including Landsat 5 TM, Landsat 7 ETM+, Landsat 8 OLI, and Landsat 9 OLI) is used, with a revisit period of 16 days and a spatial resolution of 30 m. These data are complemented by Sentinel-2 imagery, which has a nominal revisit period of 10 days and a spatial resolution of 10 m.

Meteorological and ancillary data: Monthly precipitation, air temperature, and evapotranspiration data for Ruoqiang County and Qiemo County for the period 2005–2025 were obtained from the China Meteorological Science Data Sharing Service. Additional information on cultivated land area, gross domestic product (GDP), and population was derived from the Xinjiang Statistical Yearbook.

2.3. Research Methods

2.3.1. Water Body Area Extraction

Random Forest is a machine learning algorithm based on ensemble learning principles, which has shown outstanding performance in areas such as remote sensing image classification, environmental monitoring, and ecological assessment. In this study, Lake Taitema is chosen as the study area, and the Random Forest algorithm is employed in conjunction with raw spectral bands and various water indices, including MNDWI, AWEIsh, MBWI, and LSWI, to construct a water body extraction model for dynamic monitoring of water body area over a long time series. The expressions for the water indices are as follows:

$$\mathrm{MNDWI} = \left(\rho_{\mathrm{green}} - \rho_{\mathrm{NIR}}\right) / \left(\rho_{\mathrm{green}} + \rho_{\mathrm{NIR}}\right) \quad (1)$$

$$\mathrm{AWEI_{sh}} = 4 \times \left(\rho_{\mathrm{green}} - \rho_{\mathrm{SWIR1}}\right) - \left(0.25 \times \rho_{\mathrm{NIR}} + 2.75 \times \rho_{\mathrm{SWIR2}}\right) \quad (2)$$

$$\mathrm{MBWI} = 2\rho_{\mathrm{green}} - \rho_{\mathrm{red}} - \rho_{\mathrm{NIR}} - \rho_{\mathrm{SWIR1}} - \rho_{\mathrm{SWIR2}} \quad (3)$$

$$\mathrm{LSWI} = \left(\rho_{\mathrm{NIR}} - \rho_{\mathrm{SWIR1}}\right) / \left(\rho_{\mathrm{NIR}} + \rho_{\mathrm{SWIR1}}\right) \quad (4)$$

High-resolution historical imagery from Google Earth was used to manually select sample points through visual interpretation and to label them as water or non-water. Water samples—including perennial water bodies (main lake area) and seasonal inundation zones (littoral marshes)—totaled 2000 points. Non-water samples—including bare land, saline–alkali soil, desert vegetation, and built-up land—also totaled 2000 points, ensuring a spatially uniform distribution relative to the water samples. After multiple trials, the number of decision trees was set to 150. The 4000 samples were randomly divided into a training set (2800 samples) and a validation set (1200 samples) at a ratio of 7:3; the training set was used for model parameter optimization, while the validation set was used to assess model accuracy.

2.3.2. Water Inundation Frequency

Water inundation frequency is a key metric in hydrology and remote sensing used to quantify how often, or for how long, a given area is covered by water within a specified period. Unlike static water body maps derived from a single time point, inundation frequency captures the dynamic pattern of water coverage over time. In this study, based on water body distributions extracted from long-term remote sensing imagery, inundation frequency is quantified by calculating the proportion of times each pixel is inundated during the study period. The calculation formula is as follows:

$$\mathrm{WIF} = \frac{\sum_{i=1}^{\mathrm{N}} \mathrm{w}}{\mathrm{N}} \times 100\% \tag{5}$$

In the formula, N represents the total number of valid observations for the pixel during the study period, and w denotes the number of observations in which the pixel was classified as water (The WIF value ranges from 0% to 100%).

2.3.3. Mann–Kendall (MK) Test

The Mann–Kendall (MK) test is a non-parametric statistical method primarily used to detect significant monotonic (upward or downward) trends in time series data. It is particularly suitable for datasets that do not follow a normal distribution, contain missing values, or include outliers, making it a classical tool for quantifying temporal trends in environmental science and geography. Considering that the Mann–Kendall test is sensitive to autocorrelation in time series, the autocorrelation characteristics of the analyzed variables were examined prior to trend detection. The results indicate that no statistically significant persistence was observed at the commonly used lag-1 autocorrelation scale; therefore, the application of the classical Mann–Kendall test is considered appropriate in this study. Based on this method, the Kendall's Si statistic is constructed as follows:

$$S_i = \sum^{n-1} \sum^{n} sgn(x_j - x_k) \tag{6}$$

In the formula, $1 \le i, j \le n; sgn(x_j - x_k)$ is the signum function, which takes the value of 1, 0, or −1 based on the sign of $x_j - x_k$:

$$sgn(x_j - x_k) = \begin{cases} 1 x_j - x_k > 0 \\ 0 x_j - x_k = 0 \\ -1 x_j - x_k < 0 \end{cases} \tag{7}$$

The variance of S is calculated as follows:

$$Var(S_i) = \frac{n(n\ -\ 1)(2n\ +\ 5)\ -\ \sum_{i=1}^{g} t_i(t_i\ -\ 1)(2t_i\ +\ 5)}{18} \tag{8}$$

In the formula, g represents the number of tied groups in the dataset, and t_i denotes the number of data points in the *i*-th tied group. The standardized test statistic Z_S is then calculated as follows:

$$Z_S = \begin{cases} \frac{S-1}{\sqrt{Var(S)}} S > 0 \\ 0 S = 0 \\ \frac{S+1}{\sqrt{Var(S)}} < 0 \end{cases} \tag{9}$$

A positive value of Z_S indicates a significant upward trend in the time series, whereas a negative value suggests a significant downward trend. The calculated standardized statistic Z is compared against the critical value $Z_{1-\alpha/2}$ from the standard normal distribution at a predetermined significance level α. For instance, when α = 0.05, $Z_{1-\alpha/2}$ = 1.96, and

when $\alpha = 0.01$,$Z_{1-\alpha/2} = 2.58$. If the absolute value of exceeds the corresponding critical value, the time series is considered to exhibit a statistically significant trend. Conversely, if $|Z_S| \leq Z_{1-\alpha/2}$, the trend is deemed statistically non-significant.

2.3.4. Regression Analysis

To quantitatively characterize both the temporal evolution of lake area and its response to inflow variations, regression analysis was applied in this study, including linear and nonlinear regression approaches.

Linear regression analysis based on the ordinary least squares (OLS) method was employed to quantify the rate of temporal change in lake surface area. The regression equations were used to describe long-term variation trends, and the statistical significance of the regression slopes was evaluated using *t*-tests. The goodness of fit of the linear models was assessed by the coefficient of determination (R^2). Linear regression analysis was applied as a complementary method to the Mann–Kendall test, providing a quantitative measure of trend magnitude in addition to trend significance.

In addition, nonlinear regression analysis was conducted to explore the relationship between inflow volume and lake surface area. This relationship was described using empirical polynomial functions to capture the complex and nonlinear variation pattern of lake area with increasing inflow. Polynomial regression was adopted primarily for curve smoothing and shape description, allowing the identification of nonlinear features such as inflection points and threshold-like responses. The regression parameters were estimated using the least-squares method. It should be noted that the polynomial regression was not intended for statistical significance testing or parameter inference; instead, it was used solely to illustrate the overall nonlinear form of the inflow–area relationship. Quantitative assessments of relationship strength and significance were based on linear or other parsimonious regression models.

2.3.5. Water Extraction Verification

In this study, visual interpretation results from Landsat and Sentinel satellite imagery were used as the primary reference benchmark to evaluate the accuracy of water body extraction using the Random Forest model and the index-threshold methods. A total of 300 sampling points were randomly distributed across the imagery based on spatial features, and each point was classified as either "water" or "non-water" according to the visual interpretation results, forming the standard reference dataset. Subsequently, the water body extraction results obtained from each method were matched with the reference samples corresponding to the same time periods to construct confusion matrices. Overall Accuracy and the Kappa coefficient were selected as the key evaluation metrics, where Overall Accuracy reflects the proportion of correctly classified samples, and the Kappa coefficient further quantifies the agreement between the extraction results and actual surface conditions. Through the calculation and analysis of these two metrics, the accuracy of the water body extraction results was quantitatively assessed.

3. Results

3.1. Monitoring of Lake Surface Changes in Lake Taitema, 2005–2025

3.1.1. Monthly Changes in the Lake Surface Area of Taitema Lake, 2005–2025

From 2005 to 2025, the surface area of Lake Taitema exhibited pronounced variability at both interannual and intra-annual scales (Figure 2). The long-term time series reveals a statistically significant upward trend, as indicated by the Mann–Kendall test ($Zs = 4.32$, $p < 0.001$), suggesting a persistent increase in lake extent over the study period. To further quantify the rate of change, a linear regression analysis was applied, yielding a positive

slope (y = 0.5105x + 84.596). However, the relatively low coefficient of determination (R^2 = 0.144) and the marginal significance of the regression slope (p = 0.099) indicate that linear trends alone cannot fully capture the complex temporal dynamics of lake area variation. Extreme fluctuations were observed during the study period. The maximum lake area occurred in October 2017 (461.52 km^2), whereas the minimum was recorded in October 2008 (0.35 km^2). At the intra-annual scale, seasonal variability was also substantial. For example, in 2016, the difference between the annual maximum and minimum lake areas reached 362.55 km^2, highlighting the strong seasonal expansion–shrinkage cycle.

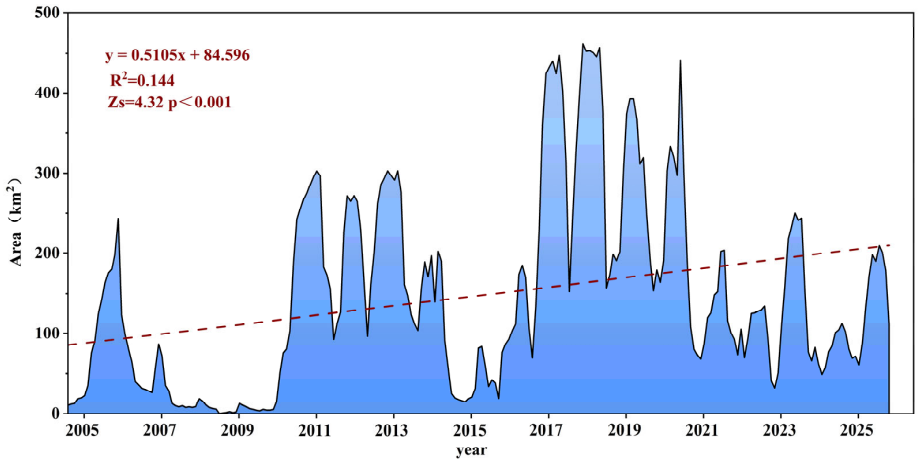


Figure 2. Variations in the water area of Taitema Lake during 2005–2025.

These results demonstrate that Lake Taitema, as a terminal lake jointly influenced by multi-source inflows and ecological water conveyance, is highly sensitive to seasonal hydrological inputs and human-regulated water allocation. While pronounced seasonal fluctuations dominate short-term lake area dynamics, the statistically significant monotonic trend detected by the Mann–Kendall test suggests that sustained ecological water management and upstream inflow regulation have contributed to a gradual long-term recovery of the lake surface area.

3.1.2. Annual Average Changes in the Lake Surface Area of Taitema Lake, 2005–2024

Based on the variations in the annual mean lake area from 2005 to 2024 (Figure 3), the hydrological evolution of Lake Taitema can be divided into three distinct stages: an expansion stage, a rapid shrinkage stage, and a stabilization stage.

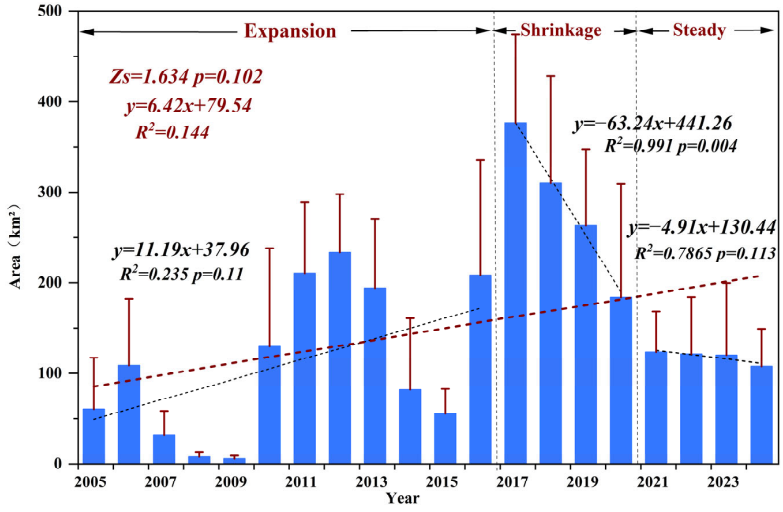


Figure 3. Annual mean lake area of Lake Taitema, 2005–2024.

(1) Expansion stage (2005–2016)

During this period, the lake surface exhibited a fluctuating yet overall increasing trend. The smallest annual mean area occurred in 2009 (5.59 km^2), while the largest value was recorded in 2012 (233.46 km^2). The pronounced interannual fluctuations during this phase were closely associated with substantial variability in inflow volumes from the Tarim River and the Qarqan River, whose discharge processes themselves are characterized by instability and irregularity.

(2) Rapid shrinkage stage (2017–2020)

This period witnessed a dramatic decline in lake surface area. In 2017, both rivers entered a wet year, resulting in a historically high inflow volume to Lake Taitema (a total of 572 × 10^6 m^3, including 359 × 10^6 m^3 from the Tarim River and 213 × 10^6 m^3 from the Qarqan River). Consequently, the annual mean lake area reached its peak at 377.10 km^2. However, beginning in 2018, as inflow volumes rapidly decreased, the mean lake area shrank correspondingly, declining to 184.33 km^2 by 2020. This stage highlights the high sensitivity of the lake extent to changes in river inflow.

(3) Stabilization stage (2021–2024)

From 2021 onward, the lake surface entered a relatively stable phase, remaining at approximately 120 km^2 for four consecutive years. This suggests that a new hydrological equilibrium has gradually formed between water inflow and evapotranspiration, indicating that the lake system has transitioned into a relatively steady state.

3.1.3. Monthly Average Changes in the Lake Surface Area of Taitema Lake, 2005–2024

Because Lake Taitema exhibits pronounced intra-annual variability, monthly lake area observations were further used for detailed analysis (Figure 4). Based on the monthly mean lake surface area, the highest value occurs in March (198.33 km^2), while the lowest appears in June (88.66 km^2). Overall, the lake surface shows a slight increase from January to March, rising by approximately 20 km^2 and reaching a seasonal peak in March. From April to June, the lake shrinks rapidly, with about 100 km^2 of water surface lost within three months, resulting in the lowest extent of the year in June. During the period from July to December, under the gradually increasing influence of ecological water releases from the Tarim River and supplemental inflow from the Qarqan River, the lake begins to recover and expands continuously, with an average monthly increase of around 15 km^2, eventually forming the second annual high-water period in winter.

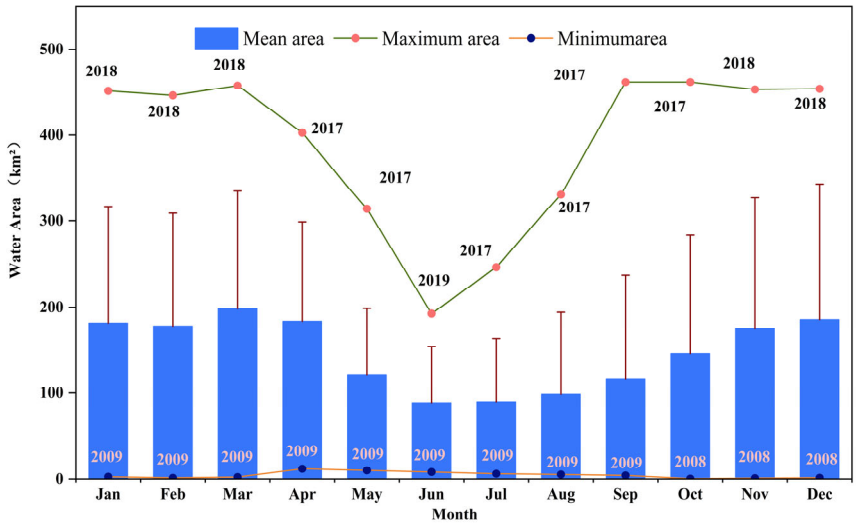


Figure 4. Monthly maximum, minimum and mean water area in Taitema Lake from 2005 to 2024 (The number on the line is the corresponding year of occurrence).

3.1.4. Lake Surface Change Features of Taitema Lake

Over the past two decades, the interannual variations in Lake Taitema have exhibited pronounced irregularity and are strongly driven by external forcing. As illustrated in Figure 5 and Table 1, the annual inflow volumes from the Tarim River and the Qarqan River fluctuate substantially and show no consistent pattern. This instability mainly stems from two factors: (1) The ecological water releases from the Daxihaizi Reservoir on the Tarim River are highly dependent on glacier meltwater and upstream water consumption. In extremely dry years, ecological releases may fail to reach the lake, whereas in wet years, only two months of releases can rapidly induce a lake surface expansion of 100–200 km^2. (2) The annual runoff of the Qarqan River is primarily controlled by glacier melt in the Kunlun Mountains, and the pronounced year-to-year differences in meltwater lead to alternating wet and dry runoff conditions, with wet years accounting for 29% and dry years for 48%. Therefore, the remarkable irregularity of lake area variability at the interannual scale essentially reflects the high uncertainty in inflow volumes and the year-specific wet–dry combinations of the two rivers, which are jointly influenced by climate-driven processes (precipitation and glacier melt) and human regulation (ecological water conveyance) along the lower Tarim River.

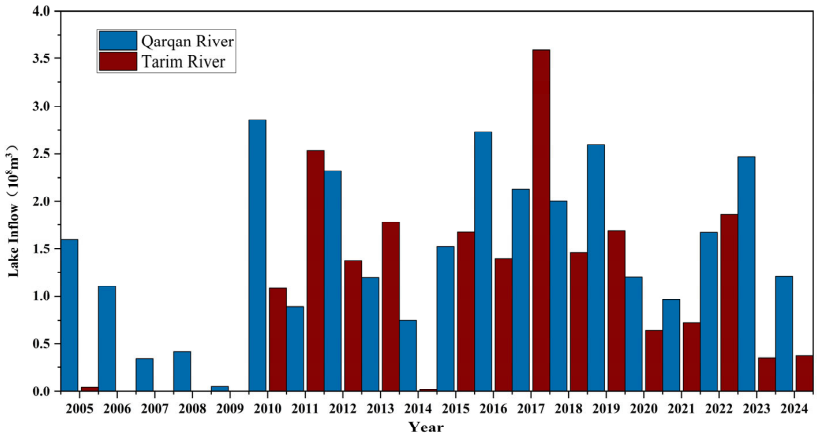


Figure 5. Annual inflow volumes from the Tarim River and Qarqan River to Lake Taitema during 2005–2024.

Table 1. Inflow volumes from the Tarim and Qarqan rivers over 20 years.

Year	Tarim River Inflow Volume (10^8 m^3)	Qarqan River Inflow Volume (10^8 m^3)	Total Inflow Volume (10^8 m^3)
2005–2014	6.84	11.53	18.37
2015–2024	13.70	20.21	33.91
Total (Proportion%)	20.54 (39.29%)	31.74 (60.71%)	52.28

In contrast, the intra-annual dynamics of Lake Taitema exhibit markedly different characteristics. Although the magnitude of lake area change within a single year is substantial (averaging 191 km^2), the fluctuations display a clear periodic pattern (Figure 6). From April to July, extremely high evapotranspiration in the arid region (2500–3000 mm per year), combined with the shallow and gently sloping basin morphology of Lake Taitema (average water depth only 0.4–0.6 m), results in rapid lake shrinkage at a rate of approximately 40–50 km^2 per month. Beginning in August, ecological water releases from the Tarim River together with seasonal flood discharge from the Qarqan River increase sharply, causing the lake surface to expand again, with an average monthly increase of about 15 km^2. During certain months when flood peaks from both rivers coincide, the lake can expand by up to 130 km^2. Therefore, the intra-annual changes in Lake Taitema are characterized by "large amplitude and pronounced periodicity," reflecting a seasonal balance between hydrological inputs and evaporative losses.

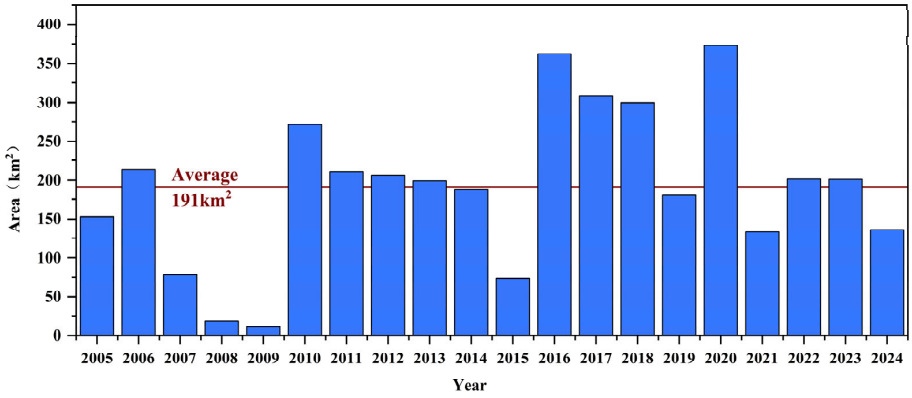


Figure 6. Intra-annual differences in the lake surface area of Lake Taitema 2005–2024.

Based on the annual maximum and minimum water extents of Lake Taitema shown in Figures 7 and 8, its spatial variation characteristics can be preliminarily examined. Over the past two decades, the minimum lake area most frequently occurred between June and August, when intense summer evaporation caused nearly all shallow-water zones to dry up, leaving only the deep-water region near the Qarqan River inflow with a persistent water surface. In contrast, the maximum lake area typically appeared in April and December, yet the spatial configuration of water bodies varied significantly among different years. This phenomenon is consistent with the preceding analysis, indicating that the differences in annual inflow volumes from the two rivers fundamentally determine the spatial distribution pattern of Lake Taitema.

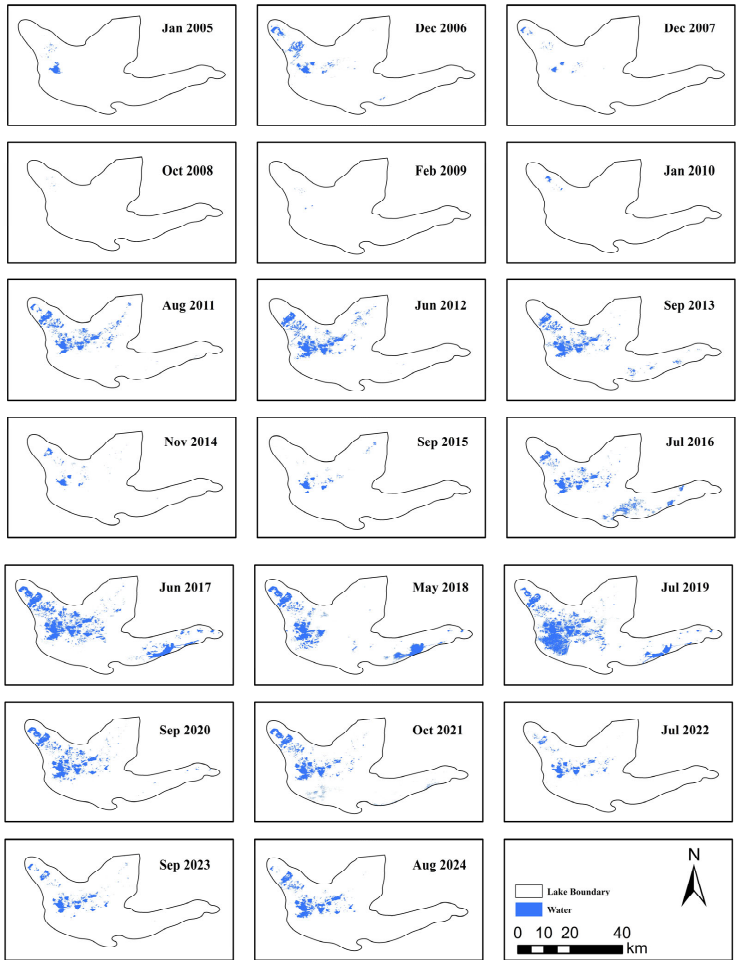


Figure 7. Annual minimum surface area of Lake Taitema during the period 2005–2024.

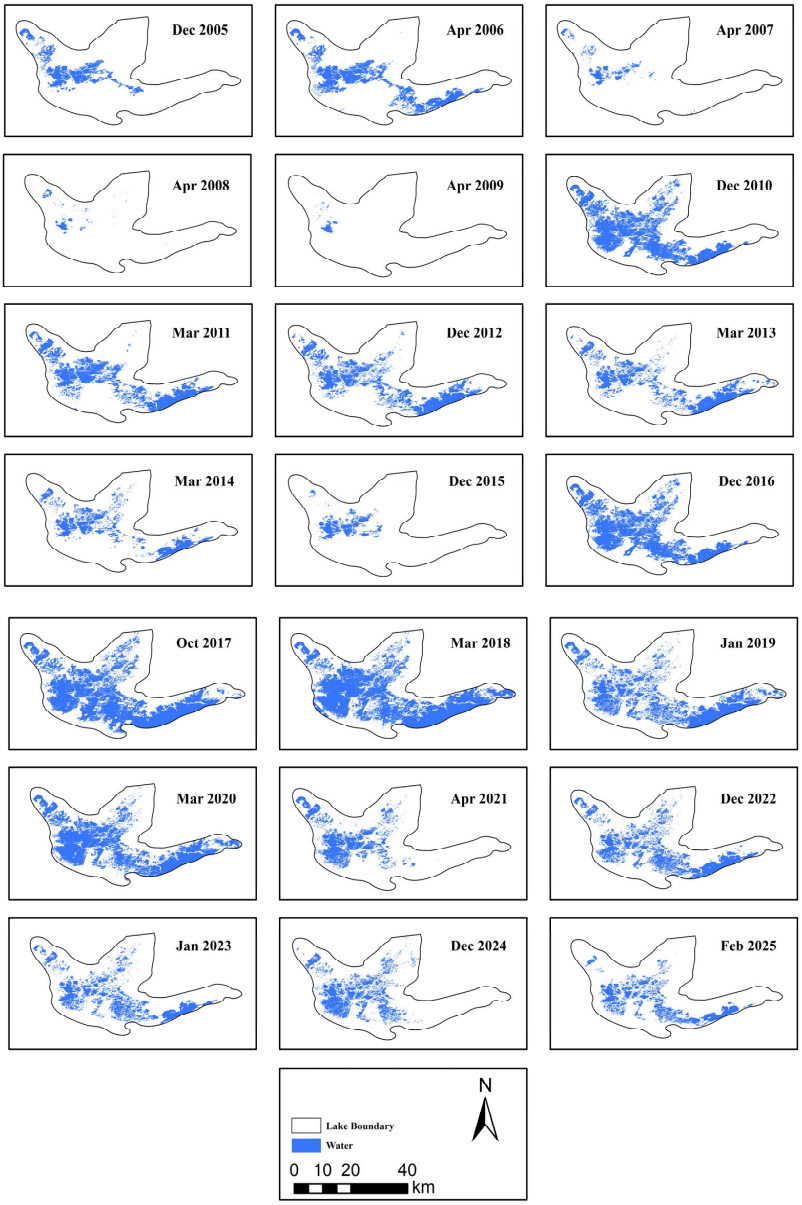


Figure 8. Annual maximum surface area of Lake Taitema during the period 2005–2025.

3.2. Water Inundation Frequency Analysis of Lake Taitema, 2005–2025

To investigate the spatial heterogeneity and temporal evolution of the lake surface in Taitema Lake, this study applied the Water Inundation Frequency (WIF) index to analyze the spatial distribution of surface water from 2005 to 2025. Considering that hydrological variations in the basin exhibit clear stage-dependent characteristics, the study period was divided into two decadal intervals. For each interval, the inundation frequency of different subregions of the lake was calculated in order to identify the dominant spatial units of lake change and to locate the core zones of perennial water.

WIF represents the probability that a given area is inundated during the statistical period. Higher WIF values indicate long-term water coverage and greater hydrological stability, while lower values reflect greater sensitivity to hydrological fluctuations and stronger spatial variability. In Figure 9, the color gradient from dark blue to deep red corresponds to low-to-high inundation frequency, respectively.

Given the pronounced intra-annual fluctuations in water level within Taitema Lake, areas with a WIF greater than 50% were defined as high-frequency permanent water bodies

(hereafter referred to as "permanent water"), representing the most stable and persistent deep-water zones. Areas with a WIF between 5% and 50% were classified as low-frequency seasonal water bodies (hereafter referred to as "seasonal water"), corresponding to shallow regions that are highly responsive to variations in inflow and are prone to exposure during dry periods.

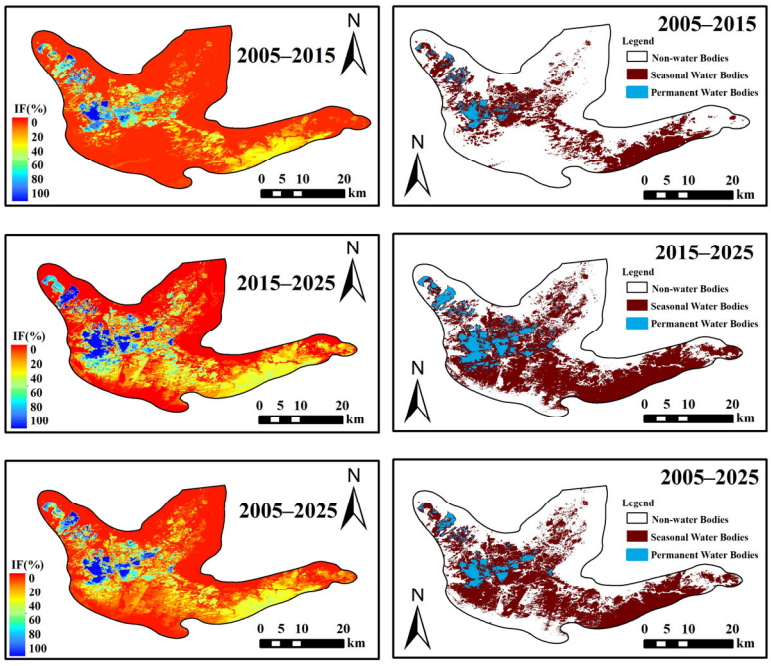


Figure 9. Water inundation frequency maps (left column) and corresponding water body distribution maps (right column) for different periods, 2005–2025.

From 2005 to 2015, the total inundated area of Lake Taitema was 251.18 km^2, which increased markedly to 400.52 km^2 during 2015–2025. Over the same periods, the extent of permanent water bodies expanded from 32.94 km^2 to 66.27 km^2, while seasonal water bodies grew more substantially, from 218.24 km^2 to 334.25 km^2 (Figure 10). This indicates that long-term ecological water conveyance primarily contributed to the expansion of seasonal shallow-water zones, while the deep-water core area also experienced gradual recovery.

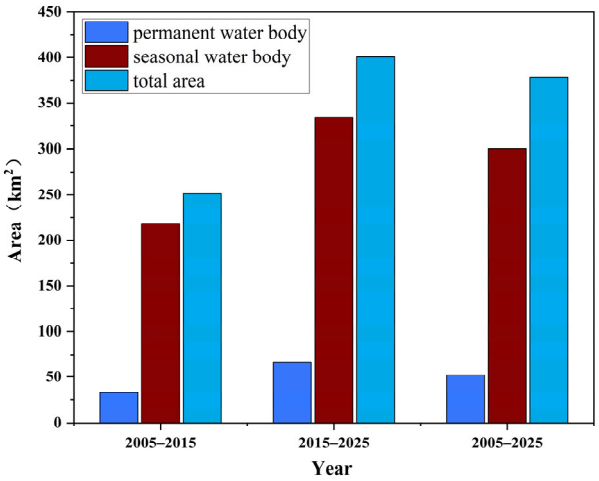


Figure 10. Area of permanent, seasonal, and total water bodies.

To more intuitively capture the spatial characteristics of lake expansion, the study area was divided into eight directional sectors at 45° intervals—north, northeast, east, southeast, south, southwest, west, and northwest—using the lake centroid as the center. The spatial evolution of different water body types was then quantified, and a petal chart was constructed to visualize directional changes across the two periods (Figure 11).

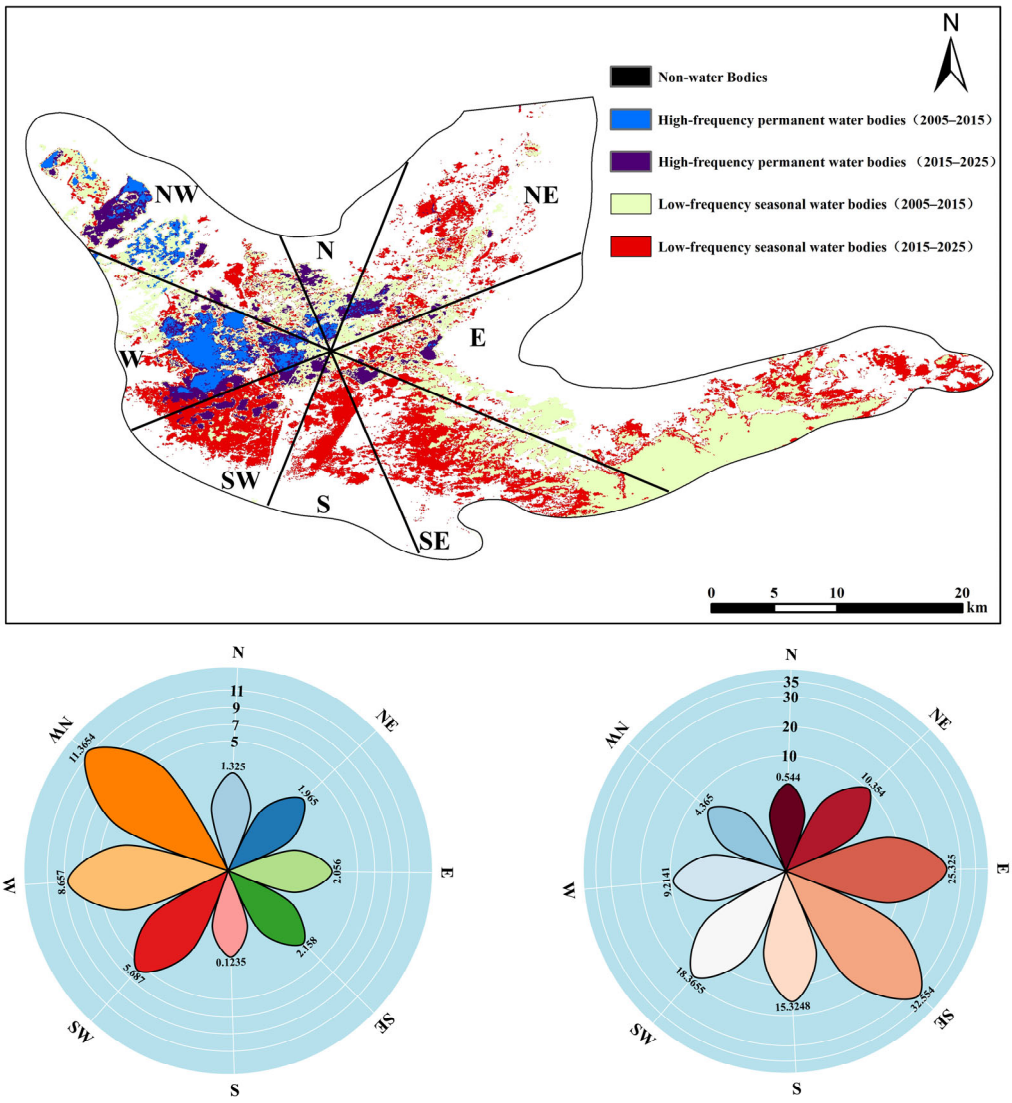


Figure 11. Changes in permanent and seasonal water areas in different directions.

Between 2015–2025 and 2005–2015, the permanent water area expanded by 33.33 km^2. The most notable expansion occurred toward the northwest, west, and southwest sectors, with increases of 11.37 km^2, 8.66 km^2, and 5.69 km^2, respectively. Together, these three directions accounted for 25.72 km^2—representing 77.17% of the total increase in permanent water bodies. This pattern reflects the deepening and stabilization of water coverage primarily around the Qarqan River inflow zone.

Seasonal water bodies increased by 116.01 km^2 during the same period. The northeast, east, southeast, south, and southwest directions showed increases of 10.35 km^2, 25.33 km^2, 32.55 km^2, 15.32 km^2, and 18.37 km^2, respectively—collectively contributing 101.92 km^2, or 87.85% of the total increase. This expansion trend is consistent with the spatial spread of shallow-water zones and floodplain inundation paths driven by ecological water releases from the Tarim River.

3.3. Lake Surface Evolution and Control Zonation by the Two Rivers

The complex spatial pattern of lake surface expansion in Lake Taitema is closely linked to the inflow volumes of its two contributing rivers—the Tarim River and the Qarqan River. To identify the spatial response mechanisms of lake expansion under different water supply sources, representative hydrological years were selected, and time-series remote sensing was used to separately reconstruct the inflow-driven lake surface evolution of each river. In addition, scatter relationships between inflow volume and lake surface area were constructed and quantified using polynomial regression to evaluate the marginal lake area increment induced by unit water inflow.

A typical Tarim-dominated hydrological process from July to November 2022 was selected, during which high-resolution Landsat and Sentinel-2 imagery were used to reconstruct lake surface changes. In July 2022, the lake surface area was only 32.21 km^2 and was confined to the deep-water zone. Because the Qarqan River inflow in that year was concentrated between late August and early September, the spatial influence of the two rivers on the lake remained largely independent, providing an ideal scenario for isolating and extracting the Tarim-controlled expansion process.

The results indicate that the Tarim-driven lake expansion can be divided into three stages. For every 0.1×10^8 m^3 of inflow, the lake surface expanded by 13.6 km^2, 7.1 km^2, and 10.7 km^2, respectively, with expansion primarily occurring across the shallow eastern half of the lake basin rather than deepening the central basin (Figure 12). These findings reveal a nonlinear sensitivity of lake surface response to staged water-input processes and provide quantitative evidence to support the development of water allocation schemes that explicitly couple inflow volumes with target lake area outcomes.

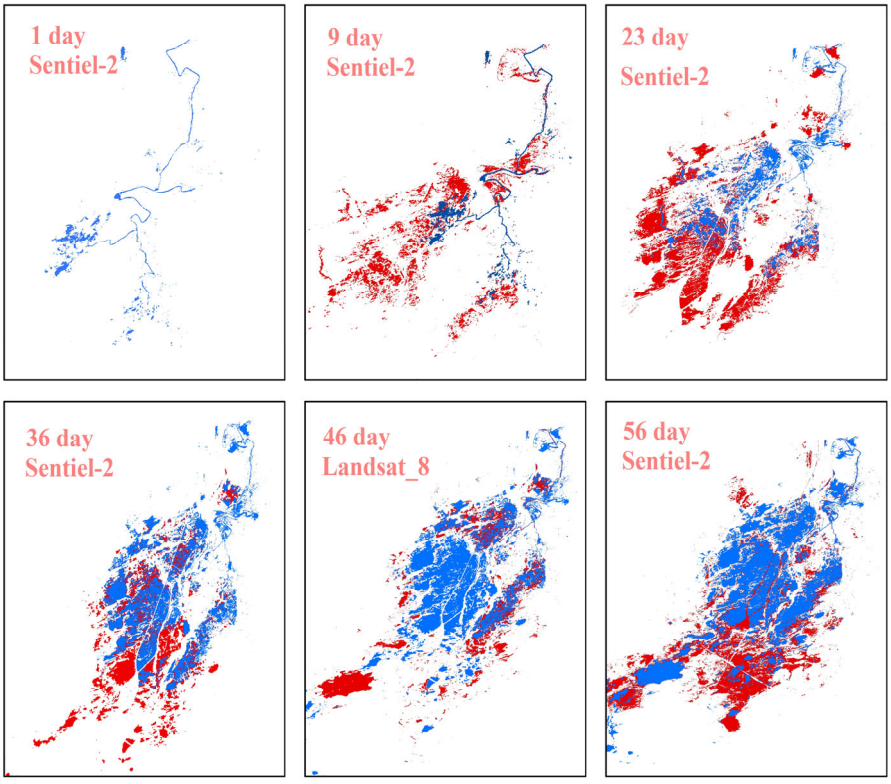


Figure 12. *Cont.*

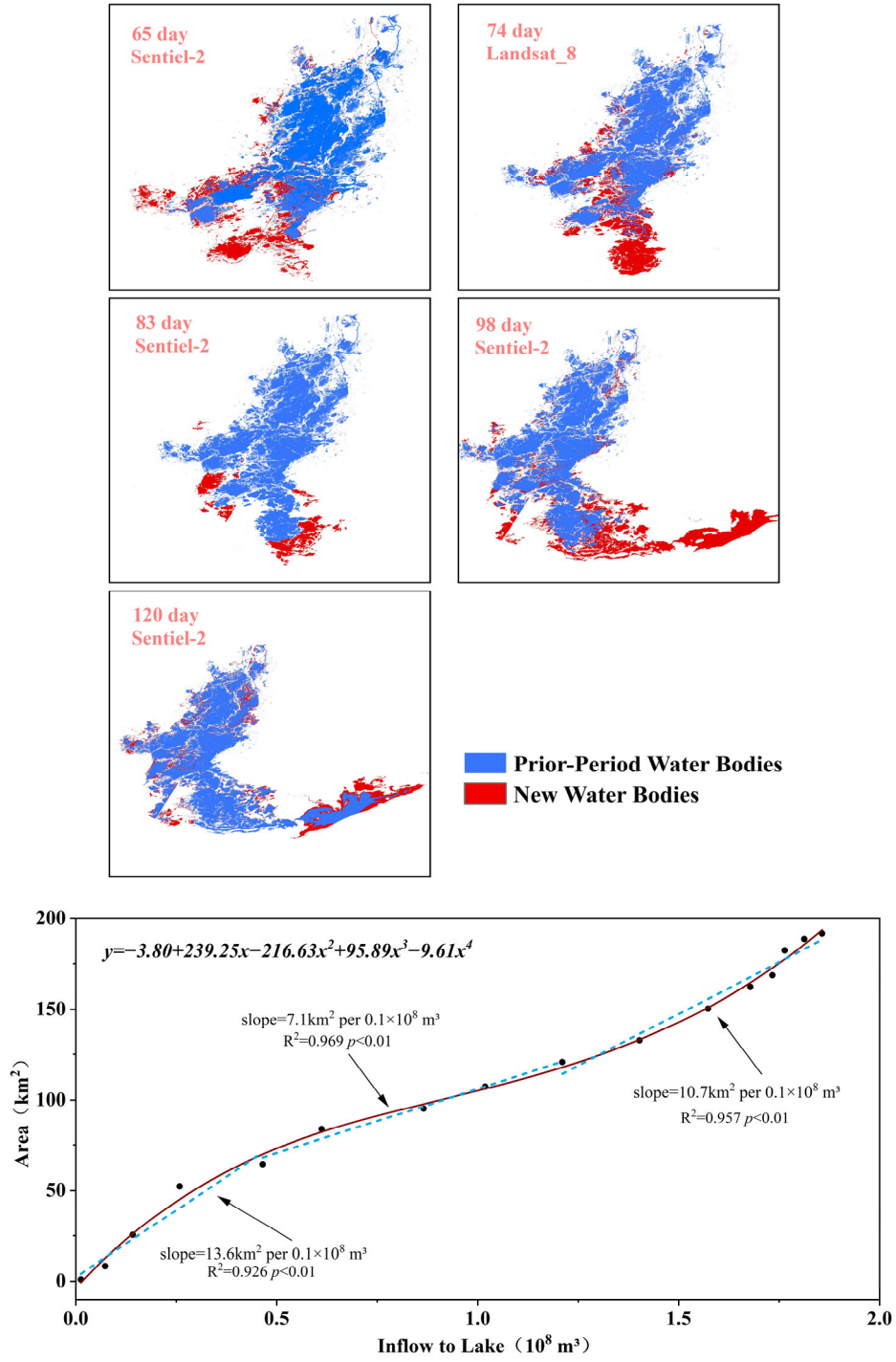


Figure 12. Variation in lake area with inflow from the Tarim River.

For the Qarqan River, representative satellite images from 2005, 2007, and 2022 (during which no Tarim River inflow occurred in 2005 and 2007) were selected to independently reconstruct the Qarqan-driven evolution of the lake surface. Similarly to the Tarim River, the Qarqan-controlled lake expansion can be divided into three stages. For every 0.1 × 10^8 m^3 of inflow, the lake surface expanded by 9.2 km^2, 4.5 km^2, and 13.5 km^2, respectively, with expansion primarily occurring within the permanent water zone as well as to its northern and southern sides (Figure 13).

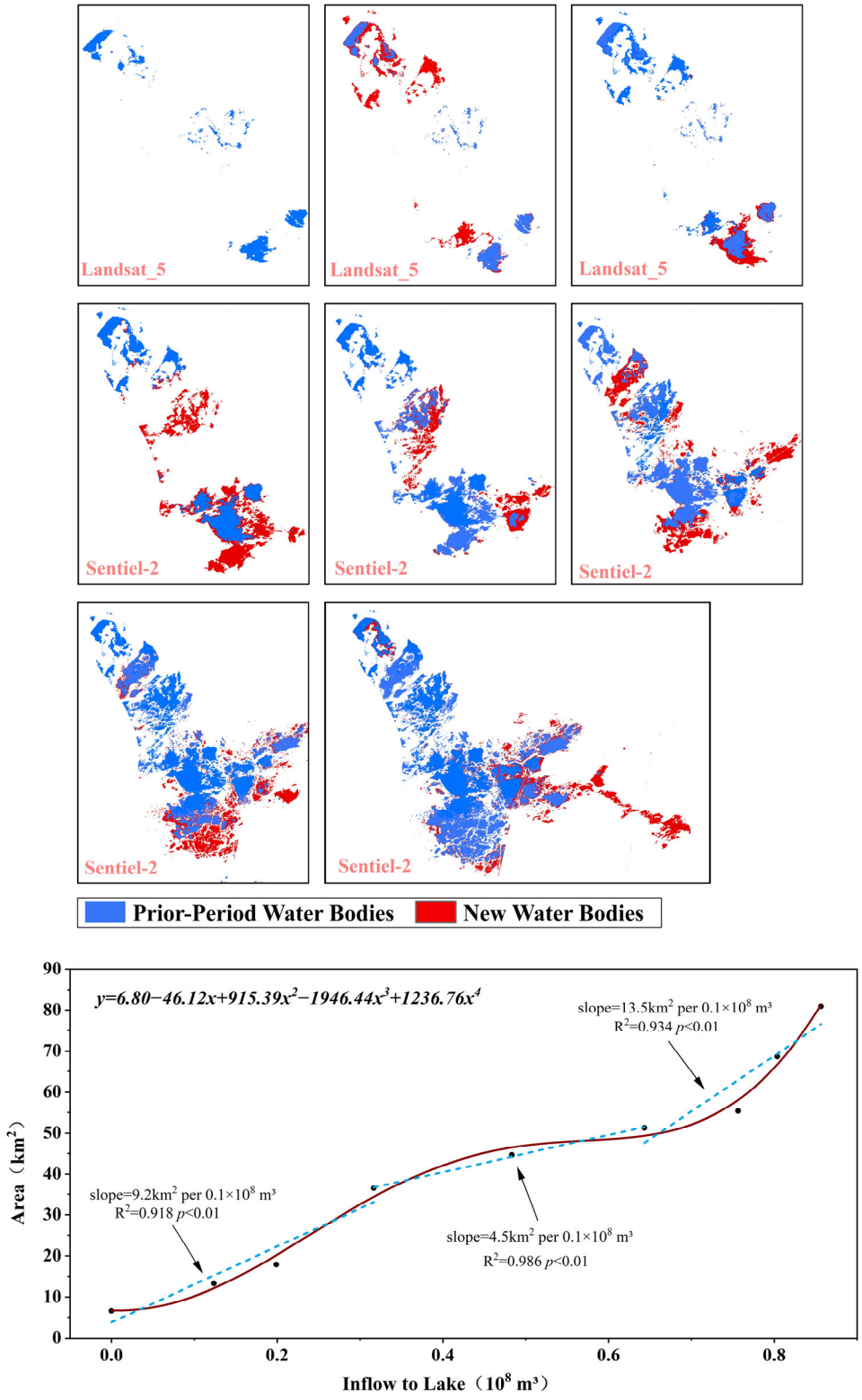


Figure 13. Variation in lake area with inflow from the Qarqan River.

Both rivers exhibit generally comparable expansion patterns; however, as inflow gradually reaches the deeper central basin, the rate of surface expansion decreases markedly, indicating a nonlinear response of lake area change to inflow volume.

Based on the high-resolution imagery and the reconstructed lake surface evolution, along with 77 additional remote-sensing scenes from other representative years, the spatial extent of the water bodies was extracted through multi-temporal superposition and visual

interpretation. This enabled the identification and delineation of the respective control zones of the Tarim River, the Qarqan River, and the jointly influenced regions of the lake (Figure 14).

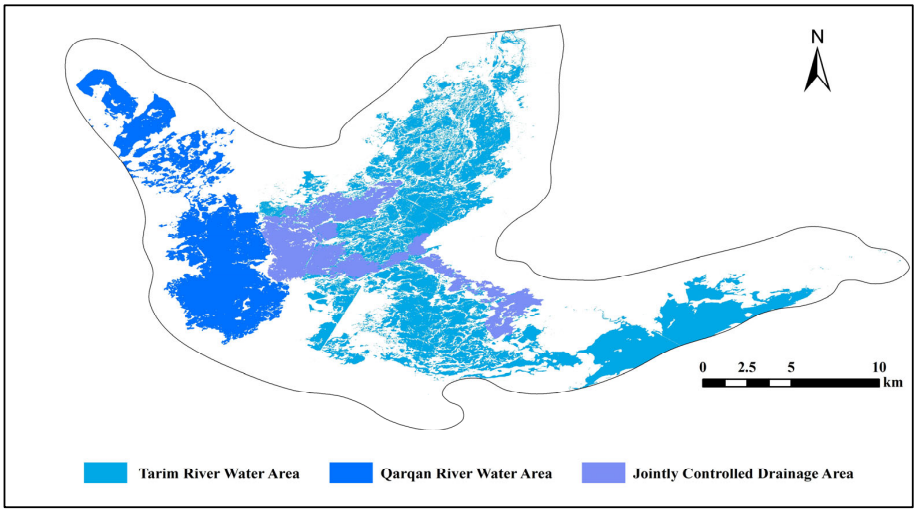


Figure 14. Respective control areas of the two rivers.

3.4. Joint Regulation Schemes for Inflows from the Two Rivers in Years of Different Occurrence Probabilities

In this section, joint inflow regulation schemes for the two rivers in years with different occurrence probabilities are developed based on the monthly lake area data of Lake Taitema from 2005 to 2025, in combination with the P-III frequency curves, the relationships between inflow from the two rivers and lake surface area, and the spatial distributions of permanent and seasonal water bodies within the lake.

According to the frequency curves and the relationships between inflow volume and lake surface area, the variation in water volume of Lake Taitema under joint regulation by the two rivers can be summarized as follows. During relatively wet lake surface conditions (P = 25%), the corresponding lake area reaches 204.34 km^2, requiring an inflow of 2.12 $\times$ 10^8 m^3. Under normal lake surface conditions (P = 50%), the corresponding area is 102.47 km^2, with a required inflow of 1.07 $\times$ 10^8 m^3. During relatively dry lake surface conditions (P = 75%), the corresponding area is 42.72 km^2, and the required inflow is 0.41 $\times$ 10^8 m^3 (Figure 15) (Table 2).

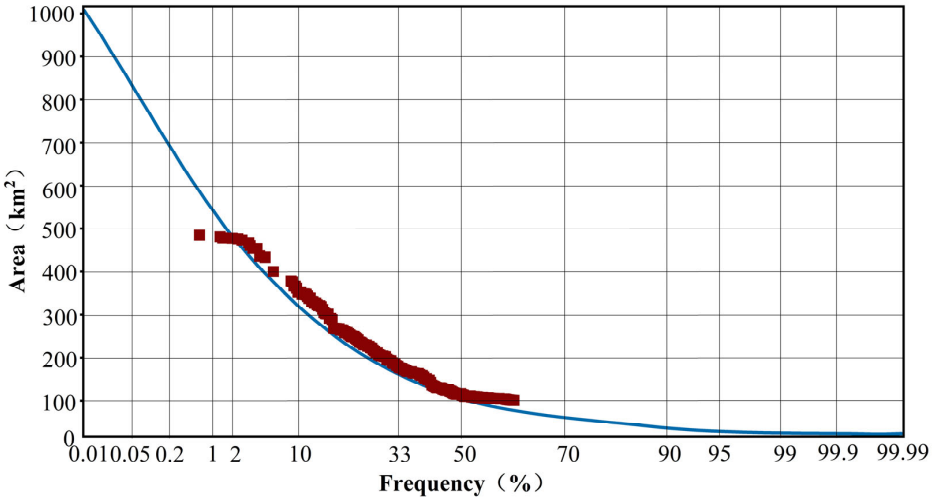


Figure 15. Frequency distribution of lake surface area in Lake Taitema.

Table 2. Lake surface area and inflow volume of Lake Taitema under different frequency conditions.

Frequency (%)	10	25	50	75	90	95
Lake surface area (km^2)	338.82	204.34	102.47	42.72	15.74	7.77
Inflow volume (10^8 m^3)	2.65	1.97	0.92	0.41	0.15	0.06

1. Lake surface protection zone and inflow scheme for relatively dry conditions;

For lake management in dry years, the high-frequency permanent water area (the deep central part of the lake) is selected as the target regulation zone. To ensure that the proposed scheme is realistic, the long-term ecological flow characteristics of the lower reaches of the Qarqan River are taken into account, and the actual inflow and scheduling scheme of the representative dry year 2007 are used as a reference. From February to April, a long-duration, low-discharge ecological release of approximately 0.25×10^8 m^3 is implemented to maintain the lake area at about 30–40 km^2. After strong evaporation during summer, an additional 0.15×10^8 m^3 of water is supplied in October to prevent desiccation of the deep central lake area (Table 3).

Table 3. Ecological inflow scheme for relatively dry lake surface conditions.

Time	Days	Inflow Volume of Qarqan River (10^8 m^3)	Inflow Discharge (m^3/s)	
			Qarqan River	Tarim River
1 February–29 February	29	0.088	3.5	0
1 March–31 March	31	0.121	4.5	0
1 April–15 April	15	0.052	4.0	0
1 October–31 October	31	0.151	5.7	0

2. Lake surface protection zone and inflow scheme for normal conditions;

For lake management in normal years, the objective is twofold: to safeguard the deep central part of the lake and to meet the water requirements of high-coverage vegetation in the lake region. To this end, a total area of 102.47 km^2, including the central lake zone and the area near the Tarim River inflow in the northeastern part of the study area, is designated as the target regulation zone. Based on the typical months of ecological water releases to the lower Tarim River over multiple years, and taking the actual scheduling scheme of the representative normal year 2020 as a reference, ecological water releases from the Tarim River are implemented from September to November. During this period, the Qarqan River continues to ensure water supply to the deep central part of the lake, with its inflow scheme kept unchanged (Table 4).

Table 4. Ecological inflow scheme for normal lake surface conditions.

Time	Days	Inflow Volume (10^8 m^3)		Inflow Discharge (m^3/s)	
		Qarqan River	Tarim River	Qarqan River	Tarim River
1 February–29 February	29	0.088	0	3.5	0
1 March–31 March	31	0.121	0	4.5	0
1 April–15 April	15	0.052	0	4.0	0
1 September–30 September	30	0	0.130	0	5
1 October–31 October	31	0.151	0.402	5.7	15
1 November–15 November	15	0	0.130	0	10

3. Lake-Surface protection zone and inflow scheme for relatively wet conditions.

For lake management in wet years, it is necessary to minimize ineffective evaporation while maximizing groundwater recharge. Building on the regulation schemes for dry and normal years and taking the actual scheduling scheme of the representative wet year 2022 as a reference, the following strategy is proposed: in spring, a long-duration, low-discharge inflow of 3.5–4.5 m^3/s is implemented to gradually expand and maintain the lake surface area at around 80 km^2; in summer, no inflow is supplied in order to reduce ineffective evaporation; in autumn, high-discharge flood-type inflows are adopted to raise groundwater levels and meet vegetation water demands, allowing the lake surface area to rapidly expand to 204.34 km^2 (Table 5).

Table 5. Ecological inflow scheme for relatively wet lake surface conditions.

Time	Days	Inflow Volume (10^8 m^3)		Inflow Discharge (m^3/s)	
		Qarqan River	Tarim River	Qarqan River	Tarim River
20 February–29 February	10	0.030	0	3.5	0
1 March–31 March	31	0.121	0	4.5	0
1 April–30 April	30	0.121	0	4.5	0
1 May–15 May	15	0.052	0	4.0	0
15 August–31 August	16	0.138	0	10	0
1 September–15 September	15	0.518	0.130	40	10
16 September–30 September	15	0.052	0.259	4	20
1 October–31 October	31	0	0.642	0	24
1 November–15 November	15	0	0.052	0	4

4. Discussion

4.1. Validation of Water Body Extraction Results

In the study area, 300 sampling points were generated following the principle of spatial randomness. Based on field observations of land surface cover characteristics and interpretation of high-resolution imagery, all sampling points were clearly classified into two categories, "water" and "non-water," thereby forming a standard sample database for accuracy validation and ensuring that the samples are representative of the surface cover types in the study area. Multiple image scenes were selected as validation benchmarks, including nine Landsat/Sentinel satellite images from different periods. For each image, water body binary maps were produced through manual visual interpretation using GIS software (version ArcGIS Desktop 10.8), and these maps were treated as the "ground truth" reference for water body extraction. The water body extraction results for each period were spatially overlaid with the corresponding visually interpreted binary maps, and point-by-point matching was performed using the 300 standard sampling points to construct confusion matrices. Based on these confusion matrices, Overall Accuracy and the Kappa coefficient were calculated. Statistical analysis of these two metrics enabled a systematic evaluation of the accuracy of the water body extraction results (Table 6).

The results show that the mean Overall Accuracy of water body extraction is 93.59%, and the mean Kappa coefficient is 0.77, indicating that the extraction accuracy meets the requirements and is generally consistent with the findings of previous studies [40]. The fluctuations in Overall Accuracy and Kappa coefficient across different periods are relatively small, and stable extraction performance is maintained at different time points. This suggests that the method is only weakly affected by factors such as seasonal hydrological variability and imaging conditions in the study area, and that it exhibits strong applicability and robustness.

Table 6. Confusion matrix for the accuracy assessment of this study.

Time	Samples	Images	Images	Total	Accuracy
		Water body	Non-water body		
September, 2005 (Landsat)	Water body	80	12	92	OA = 95%
	Non-water body	3	205	208	Kappa = 0.88
	Total	83	217	300	
		Water body	Non-water body	Total	Accuracy
November, 2005 (Landsat)	Water body	135	15	150	
	Non-water body	10	140	150	OA = 92%
	Total	145	155	300	Kappa = 0.83
		Water body	Non-water body	Total	Accuracy
March, 2007 (Landsat)	Water body	50	5	55	
	Non-water body	10	235	245	OA = 95%
	Total	60	240	300	Kappa = 0.84
		Water body	Non-water body	Total	Accuracy
July, 2007 (Landsat)	Water body	25	19	44	
	Non-water body	8	248	256	OA = 91%
	Total	33	267	300	Kappa = 0.60
		Water body	Non-water body	Total	Accuracy
April, 2014 (Landsat)	Water body	182	23	205	
	Non-water body	3	92	95	OA = 94%
	Total	185	115	300	Kappa = 0.70
		Water body	Non-water body	Total	Accuracy
October, 2022 (Landsat)	Water body	252	8	260	
	Non-water body	3	37	40	OA = 96%
	Total	255	45	300	Kappa = 0.85
		Water body	Non-water body	Total	Accuracy
November, 2022 (Sentinel)	Water body	273	6	279	
	Non-water body	8	13	21	OA = 95%
	Total	281	19	300	Kappa = 0.62
		Water body	Non-water body	Total	Accuracy
February, 2024 (Sentinel)	Water body	95	11	106	
	Non-water body	12	182	194	OA = 92%
	Total	107	193	300	Kappa = 0.83
		Water body	Non-water body	Total	Accuracy
December, 2024 (Sentinel)	Water body	267	7	274	
	Non-water body	10	16	26	OA = 94%
	Total	277	23	300	Kappa = 0.62

4.2. Spatiotemporal Zonation Characteristics and Driving Mechanisms of Lake Taitema

Existing studies consistently indicate that Lake Taitema is most sensitive to variations in water availability, whereas its direct responses to temperature fluctuations and other anthropogenic factors are relatively weak [41,42]. Most previous research has examined lake surface changes and their ecological responses primarily at the interannual scale. For example, studies have reported that since the implementation of ecological water conveyance from the Tarim River, the interannual lake surface area of Lake Taitema has exhibited a fluctuating upward trend under strong human regulation, albeit with substantial uncertainty [33]. Research on land-use change and ecological responses further shows that, compared with the pre-diversion period (1998), the lake basin in the current state (2022) has transitioned from a sand-dominated, homogeneous land-use structure to a more diversified pattern, accompanied by marked increases in vegetation coverage and water surface area and an overall improvement in the ecological environment [27,43].

These findings collectively confirm the positive role of ecological water conveyance in lake restoration from a long-term perspective. However, compared with these studies based on annual or multi-year averaged conditions, the present study refines the analytical scale to monthly and even weekly resolutions, revealing pronounced stage-dependent and nonlinear intra-annual lake surface dynamics. The results demonstrate that although interannual lake area variations are jointly controlled by inflows from the two rivers, lake expansion and shrinkage within a year follow a highly regular pattern characterized by "rapid shrinkage followed by sustained expansion." Such dynamics are often obscured when analyses rely solely on annual mean or maximum lake area metrics.

In addition, previous studies have noted that in recent years the migration rate of the lake water distribution centroid in the east–west direction has been significantly higher than that in the north–south direction, suggesting a close linkage with the hydrological processes of the east–west flowing Qarqan River [35]. By integrating Water Inundation Frequency (WIF) analysis with lake surface zonation, this study further substantiates this interpretation, clearly identifying a high-frequency permanent water region predominantly controlled by the Qarqan River and a low-frequency seasonal expansion region mainly regulated by ecological water conveyance from the Tarim River. These results reveal the differentiated spatial responses of internal lake zones to inflows from the two rivers.

In recent years, several studies have begun to examine the ecological significance of different functional zones within Lake Taitema. For instance, it has been reported that the Tarim River and the Qarqan River contribute 93.72% and 6.28%, respectively, to the hydrological connectivity of the lake, with the most critical connectivity core patches concentrated near the bridge crossing Lake Taitema, which serves as a key node within the wetland hydrological network [44]. Studies on vegetation protection priorities also indicate pronounced spatial differentiation of vegetation types within the lacustrine plain areas near the inflow termini of the two rivers [32]. These findings emphasize the ecological importance of spatial heterogeneity within the lake system. In contrast, the present study approaches lake dynamics from the perspective of hydrodynamic processes and lake surface expansion pathways. By reconstructing lake surface evolution using high-temporal-resolution remote sensing data, this study is the first to explicitly delineate, at the lake scale, the primary expansion zones controlled by each river, the permanent water core region, and the jointly controlled transitional zones. Furthermore, it quantitatively characterizes the lake area expansion efficiency associated with unit inflow volumes at different stages, thereby addressing limitations of previous annual-scale studies in capturing rapid lake responses and internal spatial differentiation.

Given that changes in lake surface area are generally governed by the coupled effects of climatic factors and human activities [45], this study selected the following variables to analyze the driving mechanisms of lake area variation in Lake Taitema: climatic factors include annual mean temperature, cumulative precipitation, and evapotranspiration (ET); human activity factors include inflow from the Qarqan River, ecological water conveyance (EWC) from the Tarim River, as well as the population, cultivated land area, and GDP of Qiemo County. Pearson correlation analysis (Figure 16) shows that lake area is strongly and positively correlated with evapotranspiration ($r = 0.84$), ecological water conveyance from the Tarim River ($r = 0.78$), and inflow from the Qarqan River ($r = 0.60$). Although the total inflow ratio of the Tarim and Qarqan rivers is 4:6, the correlation between the Tarim River EWC and the lake surface area is higher. This can be explained by the interaction between the spatial patterns of the two rivers' inflows and the lake's topographic characteristics: the Qarqan River discharges directly into the deep central basin of the lake, resulting in a relatively limited control range for surface area expansion, whereas Tarim River inflow primarily affects shallow-water zones, where lake surface area responds more

sensitively to water input and expands more rapidly. In addition, from the perspective of socioeconomic factors, the correlations of lake area with cultivated land area (r = 0.11), population (r = 0.45), and GDP (r = 0.31) of Qiemo County are weaker than those with hydrological and climatic variables, but all are positive. This indicates that, alongside regional economic development and population growth, the parallel implementation of ecological protection measures has exerted a positive driving effect on maintaining the ecological configuration of Lake Taitema.

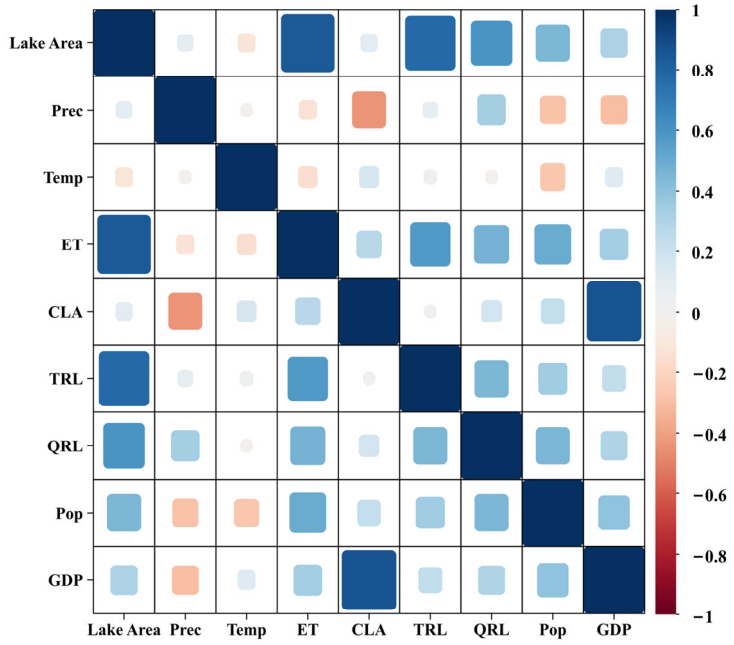


Figure 16. Correlation analysis of lake surface changes in Lake Taitema (Prec: annual cumulative precipitation; Temp: annual mean air temperature; ET: annual cumulative evapotranspiration; CLA: cultivated land area; TRL: annual inflow volume from the Tarim River; QRL: annual inflow volume from the Qarqan River; Pop: population; GDP: gross domestic product of Qiemo County).

4.3. Management Implications: Zonation-Based Joint Regulation of the Tarim and Qarqan Rivers

From a historical perspective, the recovery of Lake Taitema from complete desiccation has depended almost entirely on sustained ecological water conveyance from the Tarim River and the Qarqan River. Over the past two decades, cumulative inflows from the two rivers reached 20.54 × 10^8 m^3 and 31.74 × 10^8 m^3, respectively, forming the dominant source of lake water recovery. However, the low probability of synchronous wet–dry years (44.52%) and the high frequency of asynchronous conditions (55.48%) [6] substantially increase the uncertainty of interannual lake surface variations. Under the current context of relatively coarse ecological water conveyance and strong dependence on residual upstream water availability [46], interannual statistics alone are insufficient to support refined regulation decisions.

Lake-Surface zonation analysis reveals distinct river-specific control mechanisms. Inflows from the Qarqan River are unable to overcome local elevation gradients to supply high-coverage vegetation zones in the northeastern lake area, whereas Tarim River inflows exhibit a clear threshold effect: approximately 0.5 × 10^8 m^3 of released water is required to generate a fragmented water surface of about 65 km^2 before effective recharge reaches the permanent water region in the deep central basin. Owing to the shallow, flat, and highly fragmented lake morphology, much of the inflow is dissipated in marginal shallow areas, and only a small fraction contributes to sustaining the deep central water body.

Based on these characteristics, this study proposes a functional division of joint regulation: the Qarqan River should primarily maintain a permanent water area of approximately 30–40 km^2 throughout the year to prevent complete desiccation, while the Tarim River should mainly regulate the overall lake extent under wet, normal, and dry conditions by controlling seasonal water expansion. In essence, the Qarqan River determines whether Lake Taitema persists as a lake, whereas the Tarim River determines how large the lake becomes. The monthly–weekly lake surface response characteristics and zonation-based control framework proposed here provide a practical scientific basis for refined ecological water allocation strategies in Lake Taitema and other arid terminal lakes with multiple water sources.

4.4. Limitations and Prospects

This study still has several limitations. First, the extraction and calculation of lake surface area are based on Landsat and Sentinel remote sensing data. Although these datasets offer relatively high spatial resolution, their revisit cycles are comparatively long. During the analysis of temporal changes, some monthly images were missing because of cloud cover, adverse atmospheric conditions, and inherent data uncertainties. These gaps were filled by inferring lake surface area from adjacent months in combination with inflow data and monthly evaporation intensity, which may introduce additional uncertainty. Second, in the accuracy validation stage, only nine satellite images from different periods were selected as benchmark data. The temporal coverage and number of validation samples are therefore limited, making it difficult to fully capture water body characteristics across different hydrological seasons and during various stages of lake expansion and contraction. As a result, the accuracy assessment may not completely reflect the performance of water body extraction under more complex conditions. Third, in the analysis of lake surface evolution driven by the Tarim and Qarqan rivers, only a single special year (2022) was used for fitting, leading to a temporally constrained sample. Moreover, once the inflows from both rivers enter the common control zone, the flow boundaries and influence ranges cannot be precisely delineated, which restricts the accuracy of the fitted models and hampers a more comprehensive understanding of lake surface evolution under the combined influence of the two rivers.

In future research, it will be necessary to optimize data processing by incorporating multiple remote sensing data sources to analyze the water bodies of Lake Taitema, thereby improving the continuity, reliability, and spatial–temporal coverage of the datasets. This will provide a stronger basis for constructing a long-term, high-precision time series of lake surface area, and in turn support more in-depth analysis of the coupled driving mechanisms involving climate, hydrology, and human activities. Further clarification of the spatiotemporal patterns of lake surface changes in Lake Taitema will provide a solid scientific foundation for enhancing the efficiency of joint water resources allocation between the Tarim and Qarqan rivers and for optimizing ecological water-conveyance schemes.

5. Conclusions

- The interannual evolution of Lake Taitema can be clearly divided into three stages: an expansion period (2005–2016), a rapid shrinkage period (2017–2020), and a stabilization period (2021–2025). Spatial analysis reveals a pronounced river-controlled zonation pattern: approximately 43 km^2 of high-frequency permanent water is concentrated in the deep central basin and is primarily maintained by inflow from the Qarqan River, whereas about 300 km^2 of low-frequency seasonal water is widely distributed along shallow marginal areas and is mainly regulated by ecological water conveyance from

the Tarim River. This spatial differentiation explains the heterogeneous lake response to inflows from the two rivers.

- Furthermore, this study quantitatively establishes stage-dependent inflow–area relationships, indicating that lake surface area expands by approximately 7–14 km^2 for each additional 0.1 $\times$ 10^8 m^3 of inflow under different hydrological conditions. Based on these relationships, ecological inflow schemes for wet, normal, and dry years are proposed, directly linking target lake areas to required inflow volumes and providing a quantitative basis for coordinated regulation of the two rivers.

In summary, unlike previous studies that primarily focused on interannual scales, this study reveals rapid intra-annual lake surface responses and pronounced spatial zonation at monthly to weekly timescales. The results show that the Qarqan River mainly controls the permanent water region in the deep central basin, determining whether the lake can maintain a basic water surface during dry periods, whereas ecological water conveyance from the Tarim River primarily drives the expansion and contraction of seasonal water bodies in shallow marginal areas, thereby determining the magnitude and spatial pattern of intra-annual lake surface variations. This integrated perspective, centered on intra-annual dynamics, spatial zonation, and source-specific control, provides a scientific basis for implementing zonation-based and stage-specific ecological water regulation strategies and offers a reference for the management of other arid terminal lakes supplied by multiple water sources.

Author Contributions: S.Z.: conceptualization, methodology, software, formal analysis, writing—original draft, investigation. H.L.: supervision, resources, project administration. G.Y.: data curation, funding acquisition. Y.Z.: formal analysis. All authors have read and agreed to the published version of the manuscript.

Funding: This research was funded by the Central Guidance Fund for Local Scientific and Technological Development of Xinjiang, grant number ZYYD2025ZY22, and the Key Research and Development Project of Xinjiang, grant number 2022B03024-11.

Data Availability Statement: All data are provided as tables and figures in this article.

Conflicts of Interest: The authors declare no conflicts of interest.

References

1. Huo, T.; Yan, W.; Ma, X. A study of the variation and driving factors of the water area of the terminal lake of inland river: A case study of Taitema Lake region. *Remote Sens. Land Resour.* **2020**, *32*, 149–156.
2. Wang, J. Detection of terminal lake wetland and its landscape dynamics in arid regions:a case study from Ebinur Lake Wetland. *Acta Geod. Et. Cartogr. Sin.* **2021**, *50*, 562.
3. Huang, F.; Chunyu, X.; Zhang, D.; Chen, X.; Ochoa, C.G. A framework to assess the impact of ecological water conveyance on groundwater-dependent terrestrial ecosystems in arid inland river basins. *Sci. Total Environ.* **2020**, *709*, 136155. [CrossRef]
4. Wang, C.L.; Jiang, W.G.; Deng, Y.; Ling, Z.Y.; Deng, Y.W. Long Time Series Water Extent Analysis for SDG 6.6.1 Based on the GEE Platform: A Case Study of Dongting Lake. *IEEE J. Sel. Top. Appl. Earth Obs. Remote Sens.* **2022**, *15*, 490–503. [CrossRef]
5. Wu, F.; Yang, X.; Ren, L.; Cui, Z. Evolutionary law of hydrological and drought states in large basins of China under the influence of human activities. *J. Hydraul. Eng.* **2024**, *55*, 1448–1460.
6. Liu, K.; Chen, Y.F.; Wu, B.; Xu, H.L.; Waheed, A.; Gao, F.; He, B.; Zhou, L.; Wu, J.; Zhang, Q.; et al. Enhancing water use efficiency: Insights from hydrological variability encounter of multiple water sources and implications for terminal Lake management in arid regions. *Ecol. Indic.* **2025**, *175*, 113564. [CrossRef]
7. Bakirov, N.Z.; Novitskiy, Z.B.; Khamzaev, A.K. Methods of Creating Various Forest Plantations on the Dried-up Bottom of the Aral Sea. *Contemp. Probl. Ecol.* **2022**, *15*, 799–805. [CrossRef]
8. Feng, Q.; Endo, K.N.; Cheng, G.D. Towards sustainable development of the environmentally degraded arid rivers of China—A case study from Tarim River. *Environ. Geol.* **2001**, *41*, 229–238. [CrossRef]
9. Igor, K.; Dietz, A.J.; Ursula, G.; Anastassiya, G.; Akhan, M.; Claudia, K. Evaluation of seasonal water body extents in Central Asia over the past 27 years derived from medium-resolution remote sensing data. *Int. J. Appl. Earth Obs. Geoinf.* **2013**, *26*, 335–349.

10. Jinyue, C.; Shuisen, C.; Rao, F.; Dan, L.; Hao, J.; Chongyang, W.; Yongshi, P.; Kai, J.; Hicks, B.J. Remote Sensing Big Data for Water Environment Monitoring: Current Status, Challenges, and Future Prospects. *Earth's Future* **2022**, *10*, e2021EF002289.
11. Acharya, T.D.; Subedi, A.; Lee, D.H. Evaluation of Machine Learning Algorithms for Surface Water Extraction in a Landsat 8 Scene of Nepal. *Sensors* **2019**, *19*, 2769. [CrossRef]
12. Wang, X.; Gao, X.; Zhang, Y.; Fei, X.; Chen, Z.; Wang, J.; Zhang, Y.; Lu, X.; Zhao, H. Land-Cover Classification of Coastal Wetlands Using the RF Algorithm for Worldview-2 and Landsat 8 Images. *Remote Sens.* **2019**, *11*, 1927. [CrossRef]
13. Huang, C.; Chen, Y.; Zhang, S.; Wu, J. Detecting, Extracting, and Monitoring Surface Water From Space Using Optical Sensors: A Review. *Rev. Geophys.* **2018**, *56*, 333–360. [CrossRef]
14. DeVries, B.; Huang, C.; Armston, J.; Huang, W.; Jones, J.W.; Lang, M.W. Rapid and robust monitoring of flood events using Sentinel-1 and Landsat data on the Google Earth Engine. *Remote Sens. Environ.* **2020**, *240*, 111664. [CrossRef]
15. Su, Y.; Chen, S.; Feng, M.; Chen, F. Progress and prospects in satellite remote sensing monitoring of terrestrial surface water. *Chin. Sci. Bull.* **2024**, *69*, 3268–3282. [CrossRef]
16. Fahimeh, Y.; Mohammad, J.V.Z.; Ahmad, A.H.-B.; Alireza, B.D.; Mehdi, K.; Alireza, S. Predicting the location of larval habitats of Anopheles mosquitoes using remote sensing and soil type data. *Int. J. Appl. Earth Obs. Geoinformation.* **2022**, *108*, 102746.
17. Yao, L.; Gang, Z.; Deep, S.; Maosheng, Z.; Sudipta, S.; Sadashiva, D.; Bingjie, Z.; Shuai, Z.; Huilin, G. NASA's MODIS/VIIRS Global Water Reservoir Product Suite from Moderate Resolution Remote Sensing Data. *Remote Sens.* **2021**, *13*, 565.
18. Zhang, J.D.; Li, J.L.; Bao, A.M.; Frankl, A.; Wang, H.Y.; Bai, J.; Shen, Z.F.; Li, L.H.; De Maeyer, P.; van de Voorde, T. Ecological restoration trajectory of the Taitema Lake wetland in arid northwest China: A 36-year wetland health assessment using Landsat time series data. *Ecol. Indic.* **2024**, *161*, 111956. [CrossRef]
19. Zahra, D.; Daniel, H.; Lorena, A.; Kristinn, H.J.; Þorsteinn, S.; Dirk, T. Assessment of Landslide-Induced Geomorphological Changes in Hítardalur Valley, Iceland, Using Sentinel-1 and Sentinel-2 Data. *Appl. Sci.* **2020**, *10*, 5848. [CrossRef]
20. Lee, S.; Jeong, B.; Yoon, D.; Lee, J.; Lee, J.; Heo, J.; Lee, M.J. Quantitative Detection of Floating Debris in Inland Reservoirs Using Sentinel-1 SAR Imagery: A Case Study of Daecheong Reservoir. *Water* **2025**, *17*, 1941. [CrossRef]
21. Nagaraj, R.; Kumar, L.S. Extraction of Surface Water Bodies using Optical Remote Sensing Images: A Review. *Earth Sci. Inform.* **2024**, *17*, 893–956. [CrossRef]
22. Zhao, T.; Wu, D.; Yang, Z.; Chen, W. Evolution of coastal natural and constructed wetlands and its driving factor analysis in Guangdong-Hong Kong-Macao Greater Bay Area. *Water Resour. Prot.* **2024**, *40*, 38–47.
23. Zhao, Z.K.; Tian, Y.S.; Weng, X.X.; Li, H.W.; Sun, W.Y. Temporal and spatial variation characteristics of surface water area in the Yellow River Basin from 1986 to 2021. *J. Appl. Ecol.* **2023**, *34*, 761–769.
24. Wenjing, H.; Weili, D.; Yaning, C. Unravelling lake water storage change in Central Asia: Rapid decrease in tail-end lakes and increasing risks to water supply. *J. Hydrol.* **2022**, *614*, 128546. [CrossRef]
25. Chen, Y.; Zhang, X.; Zhu, X.; Li, W.; Zhang, Y.; Xu, H.; Zhang, H.; Chen, Y. Analysis on the ecological benefits of the stream water conveyance to the dried-up river of the lower reaches of Tarim River, China. *Sci. China Earth Sci.* **2004**, *47*, 1053–1064. [CrossRef]
26. Chen, Y.; Xu, Z. Plausible impact of global climate change on water resources in the Tarim River Basin. *Sci. China Earth Sci.* **2005**, *48*, 65–73. [CrossRef]
27. Zhang, J.; Cao, X.; Li, J. Analysis and evaluation of the ecological improvement of Taitema Lake by ecological water transport. *Res. Soil. Water Conserv.* **2025**, *32*, 316.
28. Jia, D.; Xiong, Z.; Gao, Y.; Zhang, J.; Wang, S.; Zhao, Y. Land use/land cover change and influencing factors in the Taitema Lake in the past 30 years. *Arid Land Geogr.* **2021**, *44*, 1022–1031.
29. Jiao, A.; Deng, X.; Gong, Y.; Ling, H. Increasingly enhanced water resources management effectively promotes the synergistic development of ecosystem services in inland river basins in arid regions—A case study of Tarim River. *Ecol. Indic.* **2025**, *178*, 113835. [CrossRef]
30. Jiao, A.; Xu, J.; Deng, M.; Ling, H. Vegetation net primary productivity variation characteristics and optimization path in inland river basins of arid areas driven by ecological water conveyance: A case study of the mainstream of the Tarim river. *Ecol. Indic.* **2025**, *176*, 113676. [CrossRef]
31. Kang, Z.; Ling, H.; Gong, Y.; Yan, J.; Han, F.; Shan, Q.; Zhang, G. The precise implementation of the ecological water transfer project effectively promotes the enhancement of desert riparian ecosystem service value in the mainstream of Tarim River. *Ecol. Indic.* **2024**, *169*, 112914. [CrossRef]
32. Li, X.M.; Liu, Q.; Gui, D.W.; Ci, M.T.; Liu, Y.F.; Nuerhamanti, N.; Ma, X.D. Zonation-based prioritization of vegetation conservation for terminal lakes in drylands. *Ecol. Inform.* **2024**, *79*, 102400. [CrossRef]
33. Dou, X.; Ma, X.; Huo, T.; Zhu, J.; Zhao, C. Assessment of the environmental effects of ecological water conveyance over 31 years for a terminal lake in Central Asia. *Catena* **2022**, *208*, 105725. [CrossRef]
34. Ablekim, A.; Kasimu, A.; Kurban, A.; Jappar, T.; Fan, Z. Monitoring the water area changes in Tetima-Kanglayka lakes region over the past four decades by remotely sensed data. *J. Lake Sci.* **2014**, *26*, 46–54. [CrossRef] [PubMed]

35. Zi, F.; Wang, Y.; Lu, S.; Ikhumhen, H.O.; Fang, C.; Li, X.; Wang, N.; Kuang, X. Changes in the Water Area of an Inland River Terminal Lake (Taitma Lake) Driven by Climate Change and Human Activities, 2017–2022. *Remote. Sens.* **2024**, *16*, 1703. [CrossRef]
36. Chen, Y.; Ye, Z.; Shen, Y. Desiccation of the Tarim River, Xinjiang, China, and mitigation strategy. *Quat. Int.* **2011**, *244*, 264–271. [CrossRef]
37. Hao, X.; Li, W. Impacts of ecological water conveyance on groundwater dynamics and vegetation recovery in the lower reaches of the Tarim River in northwest China. *Environ. Monit. Assess.* **2014**, *186*, 7605–7616. [CrossRef]
38. Aikeremu, A.; Abdimijit, A.; Anwar, E.; Tajiguli, K.; Shi, Z.; Alishir, K. Influence of Tarim River and Qarqan River on water area change of Tetima-Kanglayka lakes. *J. Arid Land Resour. Environ.* **2023**, *37*, 52–57.
39. Fan, Z.; Xu, H.; Zhang, P.; Zhao, X.; Abudu, L.; Fu, J. The Qarqan River in Xinjiang and Its Water Resources Utilization. *Arid Zone Res.* **2014**, *31*, 20–26.
40. Su, L.; Li, Z.; Gao, F.; Yu, M. A review of remote sensing image water extraction. *Remote Sens. Land Resour.* **2021**, *33*, 9–19.
41. Liu, Z.; Bai, T.; Gao, F.; Yang, P.; Wang, G. Optimization of reservoir operation for multi-object protection and ecosystem restoration. *Arid Zone Res.* **2022**, *39*, 410–418.
42. Hu, A.; Liu, Y.; Zhang, X.; Li, W. Ecological Water Transport and River Improvement at Lower Reaches of Tarim River. *J. Soil Water Conserv.* **2005**, *19*, 153–157.
43. Wang, H.; Tursun, K. Exploration and analysis of ecological environment change of Tetma lake before and after ecological water transfer. *Ecol. Sci.* **2020**, *39*, 93–100.
44. Wang, X.; Xu, H.; Liu, K.; Zhao, X.; Wei, G.; Aili, A.; Zheng, G. Ecological water conveyance-driven wetland hydrological connectivity and morphological changes in arid regions: An analysis of the Taitema Lake wetland. *J. Environ. Manag.* **2025**, *385*, 125615. [CrossRef]
45. Yao, C.L.; Wang, Y.J.; Chen, Y.J.; Wang, L.; Yao, J.Q.; Xia, B.F. Meteorological driving factors effecting the surface area of Ebinur Lake and determining associated trends and shifts. *Front. Environ. Sci.* **2022**, *10*, 994260. [CrossRef]
46. Lv, Z.; Li, S.; Xu, X.; Lei, J.; Peng, Z. Ecological risk assessment of landscape in arid area watersheds under ecological water conveyance: A case study of Taitema Lake. *Heliyon* **2024**, *10*, e29575. [CrossRef]

Disclaimer/Publisher's Note: The statements, opinions and data contained in all publications are solely those of the individual author(s) and contributor(s) and not of MDPI and/or the editor(s). MDPI and/or the editor(s) disclaim responsibility for any injury to people or property resulting from any ideas, methods, instructions or products referred to in the content.